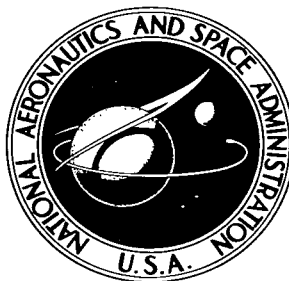


NASA TECHNICAL NOTE



NASA TN D-2235

C.1

NASA TN D-2235

LOAN COPY:

AFWL

KIRTLAND

DL54813



TECH LIBRARY KAFB, NM

SPUTTERING AT OBLIQUE ANGLES OF ION INCIDENCE

by Thomas W. Snouse

Ames Research Center

Moffett Field, Calif.



0154813

SPUTTERING AT OBLIQUE ANGLES OF ION INCIDENCE

By Thomas W. Snouse

**Ames Research Center
Moffett Field, Calif.**

NATIONAL AERONAUTICS AND SPACE ADMINISTRATION

**For sale by the Office of Technical Services, Department of Commerce,
Washington, D.C. 20230 -- Price \$0.75**

SPUTTERING AT OBLIQUE ANGLES OF ION INCIDENCE

By Thomas W. Snouse

Ames Research Center
Moffett Field, Calif.

SUMMARY

The sputtering yield and angular distributions of sputtered material were measured for obliquely incident nitrogen ions of energy 0.5 to 7.0 kev on polycrystalline copper. Sputtering yields increased in proportion to $1/\cos \alpha$ as the angle of incidence, α , increased from 0° to 60° . Angular distributions of sputtered atoms were asymmetric with a peak away from the incident ion beam at low energies, but tended to become symmetric at higher energies. The high energy distributions were peaked about the normal and were not cosine distributions.

A model of mono- and polycrystalline sputtering was constructed, based on the properties of collision events correlated because of crystal structure. The monocrystalline model qualitatively explains such phenomena as spot patterns, dependence of yield upon crystal orientation, and the decrease in yield with increasing crystal temperature. The polycrystalline model correctly predicts the observed angular distributions of sputtered material, and it also explains related phenomena such as the decrease in sputtering yield at glancing angles of ion incidence, the increase in mean kinetic energy of sputtered atoms with increased ion energies (at energies beyond the maximum yield energy), and the depth of origin of sputtered atoms.

INTRODUCTION

In an effort to delineate the mechanisms involved in the sputtering process (erosion of surfaces subjected to energetic ion bombardment), many investigators have measured the angular distributions of sputtered (ejected) material. An examination of the literature reveals, however, that considerable confusion remains because of apparent inconsistencies in the data. Specifically, the angular distributions of sputtered material have been variously reported to be cosine, and either over cosine or under cosine about the surface normal, or away from the surface normal. These terms are illustrated in figure 1. The present investigation was undertaken in an effort to resolve these inconsistencies.

In the sections to follow, the experimental results and a model of the sputtering process will be presented. The results consist of sputtering yields and angular distributions of sputtered material for polycrystalline copper bombarded by 0.5 to 7.0 kev N_2^+ ions at angles of incidence from 0° (normal to the surface) to 60° . The model will be related to the above data and the data

of others, and then applied to other aspects of sputtering, namely, the fall-off of yield at glancing angles of ion incidence, the mean kinetic energy of sputtered atoms, and the depth of origin of sputtered atoms.

EXPERIMENTAL PROCEDURE

Sputtering yields were measured by determining the weight lost by targets which had been bombarded by a known number of ions. The sputtered material was collected on celluloid, and its density, as a function of ejection angle, was measured with a microdensitometer. Further details of the apparatus and procedure are given below.

Apparatus

All measurements were made with the ion accelerators described in detail in references 1 and 2. These machines utilize a radio frequency ion source to supply a 100 to 300 μ a mass analyzed beam of positive ions of energy from 0.1 to 8 kev. The energy dispersion of the ions was small, usually less than 50 ev. The background pressures ranged from 5×10^{-6} to 5×10^{-7} torr. The ratio of the ion bombardment rate to the impingement rate of the background neutral gas molecules was generally in the range between 0.3 and 60. This is above the range where changes in yield due to ambient pressure have been noted (refs. 3 and 2) and no effects ascribable to pressure were seen. Targets appeared free of contamination after bombardment.

The target temperatures during sputtering were between 30° and 50° C. The targets were machined from electrical grade bar stock. Jeweler's rouge was used for final polish, and acetone as the final rinse. The degree of polish was not critical because the erosion rates averaged between 3 and 6 monolayers per second, and the surfaces, therefore, quickly exhibited macroscopic etching. No differences were noted in either yield or deposit pattern between measurements made with a freshly polished target and measurements made with a target having a prior sputtering history.

Yield Determination

Yields were calculated from the target weight loss, as measured by a microbalance, and the integrated current to the target, as measured by a current integrator. The reproducibility of the balance was $\pm 5 \mu$ g and the average weight removed for each data point was 1000 μ g. The integrator accuracy was ± 1 percent.

Secondary electrons were suppressed by a cylindrical electrode surrounding the target. This electrode was kept 100 to 300 volts negative with respect to the target, the lower voltage being used at lower ion energies. Visual

inspection ensured that the ion incidence angle was not perceptibly changed by the potential of the suppressor electrode.

No yield data for angles of ion incidence greater than 60° from normal are presented because of uncertainties introduced at these angles by a luminous beam seen leaving the target parallel to the target surface and in the direction away from the incident beam. This beam was not analyzed, but probably consisted of metastable gas and target atoms as well as some gas ions. These ions leaving the target make the target current measurements at glancing angles uncertain. Similar effects at higher energies, coupled with a drop in yield, have been observed by Molchanov and Tel'kovskii (ref. 4) and by Rogers (ref. 5).

The over-all accuracy of the yield measurements is estimated to be within ± 5 percent. Most of the spread in the observed data can probably be ascribed to the semimicroscopic variations in crystallite orientation on the target surface, and to the experimental difficulty of reproducing the beam shape and location on the target.

Angular Distribution of Sputtered Material

The transition from measurement of yield to measurement of angular distribution of sputtered material was accomplished by the substitution of a circular celluloid collector of radius 3.64 cm for the suppressor electrode. The circular geometry was necessary to prevent errors due to a change in the sticking probability. In early experiments with flat collectors it was found that the sticking probability of copper on celluloid decreased as glancing angles were approached. It was also found, for the neutral atom fluxes used in this experiment (averaging 4×10^{13} copper atoms per cm^2 per sec), that the initial difference in the sticking probability for a copper atom impinging on bare celluloid and one impinging on an area covered with copper made no difference in the final deposit.

The copper deposits began to oxidize after being exposed to the atmosphere for a day. For this reason, the density was measured within an hour of removal of the collector from the vacuum system.

The density of the collected deposits was measured by a double beam microdensitometer. The instrument was linear within the range of densities used, as verified by reproducing a single distribution with different over-all collector densities. If the density exceeded this range, reflections from the metallic deposit caused an incorrect density measurement. A thin deposit, on the other hand, had too little contrast and the resulting small signal from the densitometer was hard to analyze because of small shifts in the instrument's zero level, variations in the celluloid backing, and lag in the instrument. For these reasons, any individual point in the angular distribution curves may be in error by as much as 20 percent. However, these errors could not significantly shift the angular location of the maximum nor greatly affect the shape of the distribution. Duplicate experiments gave a reproducibility of 5 percent and this is taken as the over-all error of the

distributions. The 5-percent variation (considering the known influence of lattice orientation on copper sputtering yields, refs. 6, 7, and 8) can be ascribed to the shift of the ion beam from one group of crystallites to another, or the exposure of new crystallites by sputtering. Accordingly, great care was taken that the beam was small, of constant and reproducible size and shape, and extremely well centered on the target. As a further check, it may be noted that distributions obtained with normally incident ions were symmetrical.

Sputtering Yields at Oblique Angles of Ion Incidence

The sputtering yield of copper bombarded by N_2^+ is presented in figure 2 as a function of ion energy for various angles of ion incidence α . As expected, the yields increase with energy and with angle of ion incidence.

Figure 3 presents the yield data as a function of incidence angle for various ion energies. The angular yields are normalized to the 0° yield. These normalized yields are slightly below a $1/\cos \alpha$ curve (excepting the 0.5 kev case), and the departure becomes more pronounced as α increases. It is apparent that extension of these measurements would be desirable for the range $60^\circ < \alpha < 90^\circ$. Unfortunately, as mentioned previously, the experimental limitations did not allow good data to be obtained in this region.

Angular Distribution of Sputtered Material

The measured angular distributions of sputtered material are shown in figures 4, 5, and 6 as polar plots. Each distribution was normalized to its maximum, and a cosine distribution, shown by a dotted line, is included for comparison. The incident beam is indicated by an arrow.

Figure 4 illustrates the change in distribution with increasing ion energy at a constant ion incidence angle of 30° . The behavior is typical of that at other angles. The change is from decided asymmetry in figure 4(a) to an over cosine distribution in figure 4(f).

Figure 5 shows the distributions obtained at ion incidence angles of 0° , 30° , 45° , and 60° at 4 kev. Although the yield changes from 4.3 to 7.4 atoms per ion, the distribution shape remains roughly the same. Some slight asymmetry is noted in the 60° case.

Figures 6(a) and 6(b) (normally incident N_2^+ at 6 kev and 4 kev N_2^+ at 30°) are a comparison of angular distributions whose sputtering yields are nearly equal. The mean free paths normal to the surface differ by roughly 35 percent.¹ The distributions are similar, both being over cosine.

¹The mean free paths are estimated by the method of Bohr (ref. 9).

Figures 4(e) and 5(a) (5 kev N_2^+ at 30° and 4 kev N_2^+ at normal incidence) are a comparison of angular distributions whose mean free paths normal to the surface are equal. The corresponding yields are 5.2 and 4.4 atoms/ion. Once again the distributions are similar.

Figures 6(c) and 6(d) (normally incident N^+ at 5 kev and 1 kev N_2^+ at 30°) are a comparison of angular distributions whose yields are nearly equal. Because of the smaller size of the N^+ atom, the mean free path in the first case is five times as long as that in the second. The distributions are not similar, indicating that depth of penetration may be a factor in the angular distribution of sputtered material.

It may also be noted that a cosine distribution might not be obtained at any energy for some ion-metal combinations. If the 30° incident angle distributions at energies of 3, 4, and 5 kev (figs. 4 and 5) are examined, it is seen that the distributions have changed from asymmetric to symmetric by the atrophy of the asymmetric spur and the growth of the peak about the normal. This transition is apparently accomplished without passing through a cosine distribution.

Perhaps the most striking result of these experiments is the demonstration of the existence of both symmetric and asymmetric angular deposits for a single ion-metal combination. Although many angular distributions are to be found in the literature, none has been in an energy region such as to demonstrate this transition from one distribution to another. Consequently, until now, there has been some doubt that the variety of reported distributions was in any way consistent.

MODEL OF THE SPUTTERING PROCESS

This section attempts to construct a qualitative model of the sputtering process consistent with the preceding data. The immediate object is the understanding of physical situations where sputtering may occur, and not the actual calculation of measurables, although these calculations may follow as more single crystal sputtering data are obtained. The discussion will be confined to copper, but is readily extended to other substances. The model incorporates the ideas of many workers, but in general, it is most consistent with the treatment by Harrison (ref. 10).

Monocrystalline Sputtering Model

Present day momentum transfer sputtering theories, for energies on the order of 1 to 100 kev, draw the following picture. An energetic ion impinging on a metal lattice penetrates a mean distance λ before making a collision. The struck lattice atom and the ion make further collisions in the near neighborhood of the initial collision, forming a cascade of energetic lattice atoms. In turn, these energetic atoms may travel between rows of lattice atoms (as

dynamic crowdions), start a series of focusing replacement collisions (replicons), or initiate a series of focusing collisions without replacement (focusons).² Although collision processes have been treated extensively in the literature (refs. 13 through 18), the mechanics of collision processes in an ordered lattice will be reviewed briefly here since they determine the essential features of the model.

Silsbee (ref. 14) originally suggested that the lattice structure of a crystal implied a correlation between successive collisions in a damage process. He showed that, for most metals, energy focusing along a close-packed line of atoms could be expected if the criterion $d/r_0 \leq 2 \cos \beta$ was satisfied, where d/r_0 is the ratio of atomic lattice spacing to effective atomic diameter and β is the angle between the initial impact and the axis of the close-packed line. Since the effective collision cross sections decrease with increasing energy of interaction, d/r_0 increases with energy. This imposes a ceiling on the initial energy of a focuson. Liebfried (ref. 15) estimated that this energy is on the order of 63 ev for focusing in the close-packed direction in copper. The ceiling energy of a replicon is indefinite, but higher than that for a focuson, while the crowdion has no ceiling energy.

These processes are important in any theory of sputtering, since their combined effect is the transport of energy from the initial collision site for a distance greater than that predicted by simple diffusion theory. The ranges of energy transport for the collision sequences increase in this order, crowdion, replicon, focuson. As an illustration, an energetic atom might travel for 5 atomic diameters as a crowdion, losing energy by glancing collisions. It might then initiate one or several replicons of range 10 to 20 atomic diameters. In turn, as energy is lost, an interstitial may be formed, while a focuson carries the remainder of the energy for distances up to 100 atomic diameters. For examples of the above behavior, refer to Gibson, Goland, Milgram, and Vineyard (ref. 19). These workers also predicted that focusons also propagate in next nearest neighbor directions (although with reduced efficiency), a prediction that has subsequently been verified by the production of spots corresponding to these directions in single crystal deposit patterns.

These ranges are limited by the mechanisms of energy loss. For a crowdion, the principal losses are due to glancing collisions with the atoms in the rows between which the crowdion is traveling. For focusons and replicons, there are two main types of loss in a pure substance. First, as the momentum is being focused down a row of lattice atoms, the initial collisions which are at an angle to the axis of atoms will leave the original particle with some remaining momentum. Second, since a collision with the next atom in a chain occurs after the first atom has moved away from its lattice site, the first atom is left in a region of higher potential energy, with respect to its neighbors, and thus has not been able to transfer all of its initial kinetic energy.

²The names in parentheses have arisen in analogy to the phonon, since momentum is focused into certain crystal directions and is transferred by a particle or particle-like process in these directions with little attenuation. These terms will henceforth be used for the sake of brevity (refs. 11, 12, and 13).

This is true even in the case of head-on collisions. Other energy losses can arise from thermal vibration of the lattice atoms, from the presence of atoms of different atomic weight, and from defects in the lattice structure.

Sputtering occurs when a crowdion, replicon, or focuson arrives at a surface with sufficient energy remaining for the escape of a lattice atom. The escaping atom has the energy of, say, a focuson minus the sublimation energy and leaves on the average in the focusing direction.

This, in turn, implies that the number, energy, and direction of sputtered atoms are determined not by the surface properties, but by the volume properties of the material. This point cannot be too strongly emphasized, for it is the very heart of the model. Surface conditions, for example, roughness or adsorbed gases, may have a measurable effect, but it is the volume properties which control the gross features of sputtering.

A further consideration shows that ion bombardment creates two energy populations within the lattice. The first population consists of the crowdions, replicons, and focusons, which rapidly remove energy from the collision area. The second population consists of the atoms left in a state of thermal excitation by the loss mechanisms of the first population. This energy is dissipated by phonons in a time perhaps an order of magnitude longer than that taken by the processes of the first population. This thermal energy may be high enough to cause some sputtering, and Thompson and Nelson (ref. 20) give evidence, from velocity analysis of sputtered atoms, that, in certain cases, this mechanism may be responsible for some 4 to 12 percent of the total yield.

The most significant result of these considerations is the emphasis on crystal structure as a vital parameter in the sputtering process. The following phenomena provide a critical test: the deposit spot patterns obtained at all ion energies as a result of single crystal bombardment (fcc, bcc, and hcp crystals) (refs. 21 and 22), the dependence of yield upon single crystal orientation (refs. 6, 7, and 8), and the decrease in sputtering yield of polycrystalline materials with increasing temperature (refs. 23, 7, and 2). Spot patterns are readily explained by this model, since they are directly related to the focusing directions. Indeed they may have been the stimulus that led to a description of focusing phenomena (refs. 14 and 21). The variation of yield with crystal orientation follows from two considerations. First, the penetration of the ion is determined by the "transparency" of the crystal. The deeper the penetration, the lower the yield, and consequently, the most open orientations of a crystal have the lowest yields. Second, the number of collision processes reaching the surface is determined by the number of nearest and next nearest neighbor directions whose direction is out of the surface, their angle with the surface normal, and the relative efficiency of energy propagation along these axes. The decrease in yield observed as a function of temperature in the range 20° to 500° C can best be explained by noting that high temperatures reduce chaining efficiency (ref. 14) and thus reduce yield (ref. 2). Thus the model gives a qualitative explanation for behavior not predicted by theories based on the assumption of isotropic material.

Polycrystalline Sputtering Model

In order to treat the problem of polycrystalline sputtering, this single event model must be placed in a statistical framework, which appears to be justified if the orientation of crystallites in a polycrystal is truly random. It is further justified in terms of interpretation of experimental results, as a large number of impacts is necessary for a single sputtering measurement. This approach then allows the computation of the mean free path of the ion and the subsequent momentum flux probabilities on the basis of an isotropic medium. However, since an individual crystallite is larger than the volume influenced by a single impact, crystal structure still determines the momentum range and thus retains a determining role in the sputtering process.

Figure 7 is a cross-sectional schematic drawing of this sputtering model. The wavy line represents the target surface. An ion enters the surface at an angle α and penetrates a depth λ before making a collision with significant energy transfer. The mean crowdion range, R_C , then outlines a volume in which most of the cooling (the prerequisite degradation of collisional energy below the replicon and focuson ceiling energy) takes place. Because crowdion range is determined by the kinetics of the original collision, the range is a function of direction and therefore biased in the forward direction. It is represented here by an ellipsoid whose focus is placed at the point of initial collision, and whose foci are separated by $2a$. The size and shape of this volume would become two adjustable parameters in any quantitative calculations from this model.

The surface of this volume then becomes the source of replicons and focusons. Since their initial energy is limited, their range is independent of initial direction, and the large sphere of radius R illustrates this. Actually this volume must be an ellipsoid, because its generator was ellipsoidal. Since R is the sum of the focuson and replicon ranges R_F and R_R , plus a small contribution from the initial ellipsoid, and R_F and $R_R \gg R_C$, the ellipsoid may be closely approximated by a sphere centered at $\lambda + a$.

Although the range of a focuson or replicon is independent of direction, the flux is not. The momentum flux must be biased in the forward direction, and this is illustrated by the spacing of the ticks outlining the sphere of maximum range. Once again in a quantitative calculation this flux distribution must be a parameter dependent upon the energy transfer factor.

Two points should be mentioned before the close of this discussion. First, the illustration of maximum range in figure 7 should not be taken as indicating that all focusons have the maximum range. Actually isorange spheres could be drawn to indicate that some focusons or replicons began with less than the ceiling energy. Second, it may be noted that the region of thermal excitation may be treated in similar fashion, its volume spherical, of radius R_T and centered at $\lambda + a$. The order of magnitude of R_T is $R_C < R_T \ll R$.

The behavior of R as a function of incident ion energy is necessarily complex. At low energies, roughly between 0.1 and 1 kev, few replicons would

be formed, since the average energy available after the initial ion collision is in the range of the ceiling energy for focusons. Therefore $R \approx R_f$. At intermediate energies, 1 to 10 kev, the replicon range begins to extend R . When the ceiling energy for replicon formation is reached, R becomes essentially independent of energy, and it is at this point that the sputtering yield begins to decrease as a function of energy.

The model also leads to the following predictions for the distribution of material sputtered by obliquely incident ions.

1. Where ion penetration normal to the surface is small ($\lambda \cos \alpha \lesssim 1/2 R$), as would be the case at low energies or at glancing angles of incidence, an asymmetric distribution of sputtered material is expected. This is due to the large variation of the momentum flux function over the wide solid angle of focusons able to reach the surface. This is illustrated in the upper left-hand corner of figure 8.

2. At medium energies (represented by fig. 7 where $\lambda \cos \alpha \approx 3/4 R$), the asymmetries should become less noticeable because, although the surface area falling within the R sphere is larger, the solid angle subtended by the surface is smaller. Therefore the change in the momentum flux function over the surface is smaller. This change is also opposed by the shorter path length to the surface taken by normally exiting focusons. This example exhibits the maximum yield.

3. At high energies, where $\lambda \cos \alpha \lesssim R$, only those focusons arriving at angles nearly normal to the surface can cause sputtering. Therefore, the angular distribution of sputtered particles should peak about the surface normal as in the case of normal incidence sputtering. This is illustrated in figure 8, which is drawn to the same scale as figure 7.

4. Since the ion penetration is dependent upon ion and target atom's atomic number, the relative energies for transition from one type of behavior to the next must vary for each ion-metal combination. That is, a light ion incident upon a given metal should yield a symmetric distribution at a lower energy than a heavy ion upon the same metal.

COMPARISON WITH EXPERIMENT

The experimental data presented agree in all respects with the predictions of the model. As a further check the model will be compared with the angular distribution data of others. In addition we shall discuss briefly the insight given by the model into the related problems of the yield at glancing angles of ion incidence, the mean kinetic energy of sputtered atoms, and the depth of origin of sputtered atoms.

The earliest measurements of angular distribution of sputtered material were made by Seeliger and Sommermeyer (ref. 24) who found cosine distributions for 5 to 10 kev Ar^+ on silver and molten gallium at angles $\lesssim 45^\circ$. Since argon is relatively heavy, some departure from the cosine law would be expected. It

is entirely possible that the structure may have been lost because of the small (1 cm radius) size of their collecting surface. The authors remark that their results are to be considered as only a first approximation and no mention is made of any but a visual determination of deposit density.

Wehner (ref. 21) and Wehner and Rosenberg (ref. 25) obtained obliquely incident 100 to 400 ev Hg^+ on Mo and Ni in a glow discharge by bombarding the edges of a plate. Although the angles of incidence are not known, the deposit was definitely away from the incident beam, in agreement with prediction 1.

Rol, Fluit, and Kistemaker (ref. 26) found an over-cosine distribution for 20 kev Ar^+ on copper at 50° . A close examination of their distribution reveals some slight asymmetry, but over-all the result agrees with prediction 3.

Stein and Hurlbut (ref. 27) report asymmetric distributions obtained by 50 to 450 ev noble gas (He^+ , Ne^+ , Ar^+ , Xe^+ , Kr^+) bombardment of potassium at various angles. Their distributions are in good agreement with predictions 1 and 4.

Patterson and Tomlin (ref. 28) report unique distributions for 5 and 10 kev Ar^+ on gold at 20° . The distributions were very close to cosine, but with a slight peak in the beam direction. Their angular distribution results are in general agreement with prediction 2.

Grønland and Moore (ref. 29) report a cosine distribution for 4 kev Ne^+ on Ag at 60° . This is in conflict with prediction 1. Repetition of the experiment in our laboratory produced asymmetrical deposits, but we have found no explanation for the discrepancy between the two sets of results.

Pleshivtsev (ref. 30) found an asymmetric departure from the cosine distribution for 54 and 40 kev hydrogen ion beams on copper at 60° . In this extreme case of light ions at high energy, such a result does not agree with predictions 3 and 4. However, it should be noted that the unanalyzed beam contained more than 1 percent O_2^+ and N_2^+ ions formed by charge exchange at lower energy than the beam. Since this much impurity concentration is known to affect the yield data considerably (ref. 31), it probably also explains the asymmetry. However, Grønland and Moore (ref. 29) report a similar, though less pronounced, departure for 9 kev deuterons incident on silver at 60° . They advance the idea that the large (~10 percent, see ref. 32) probability for specular reflection of these light ions may allow the reflected ions to sputter a surface atom and so account for the enhanced sputtering in the forward direction.

More experimental evidence in this region would be desirable, since the limits of the model are evidently approached. This is because light ions are unable to transfer large amounts of energy in a single collision. The mean free path between the first and second collisions may be quite large and give rise to several crowdion centers rather than the single center in the simple model considered here.

It is apparent that the model offers a description of sputtering behavior that is consonant with the majority of the angular distribution evidence.

Decrease of Yield at Glancing Angles of Ion Incidence

Molchanov and Tel'kovskii (ref. 4) have measured yields as a function of angle of incidence in the case of 27 kev Ar^+ on copper. They found that the yield was proportional to $1/\cos \alpha$ until $\alpha = 66^\circ$, reached a maximum at about 75° , and fell off as the angle of incidence increased. They also measured the energy of the fast particles emitted by the target at angles close to glancing. They found that while the energy in this beam increased qualitatively with the observed falloff of yield, the quantitative agreement was not good. For example, at $\alpha = 78^\circ$ the fraction of the original beam energy reflected was 6 percent, while the deviation of the magnitude of the sputtering from $1/\cos \alpha$ was 40 percent. Dushikov, et al. (ref. 33) found that the maximum yield as a function of angle of incidence shifted to larger and larger angles as the ion mean free path increased.

This behavior is explained by noting that part of the crowdion volume may intersect the surface. Thus there is a probability that crowdions escape with sizable energies. Their escape before they have cooled reduces the number of focusons and replicons formed and thus reduces the yield.

Mean Kinetic Energy of Sputtered Atoms

Kopitzki and Stier (ref. 34) have published the results of extensive measurements of the mean kinetic energy of sputtered atoms. The cases studied were 20 to 60 kev Ne^+ , Ar^+ , Kr^+ , and Xe^+ ions incident over a range of angles on various metals. They found that the mean kinetic energy of the sputtered atoms increased with increasing ion penetration. This differs from the behavior of the sputtering yield, which, to a first approximation, is inversely dependent on the ion penetration at these energies.

This behavior is not predicted by the model if only focusons, etc., are considered, since at high ion energies, the longer focuson paths to the surface should cause mean energy to decrease. However, in this case, the atoms sputtered by thermal processes must be considered.

Since a thermally sputtered atom has energy less than 1 ev (ref. 20) compared to the ~6 to 100 ev energy of an atom sputtered by other collision mechanisms, their effect in reducing the mean kinetic energy is sizable, although they may represent less than 10 percent of the atoms sputtered.

As the penetration increases, most of the thermal excitation takes place at too great a depth to contribute to sputtering, and the mean energy of the sputtered atoms rises as a consequence.

Depth of Origin of Sputtered Atoms

The model predicts that the majority of sputtered atoms are surface atoms. However, Patterson and Tomlin (ref. 28) concluded that a large number of sputtered atoms originate from finite depths, and that these atoms are responsible for the deviations of the sputtered material from a cosine distribution.

These conclusions stemmed from two experiments involving double layered targets. The first experiment had a nonradioactive gold layer over a radioactive gold substrate. A measurement of the time of appearance of radioactive gold atoms versus the rate of removal of the surface layer of atoms presumably gave values for the crowdion range in gold. The values so obtained gave crowdion range values apparently longer than the mean free path of the ion.³ In addition, the mean ranges measured disagreed by an order of magnitude with the photoneutron reaction recoil ranges of gold nuclei in gold measured by Van Lint, et al. (ref. 37). These discrepancies may be explained by pinholes in the evaporated films or preferential sputtering of selected crystallite orientations.

Their second experiment was the measurement of the angular distribution of radioactive gold atoms sputtered from a thin layer of radioactive gold atop a nonradioactive gold substrate. Measured distributions more and more closely approached a cosine as the layer thinned. In view of the earlier remarks concerning the variability of the thickness of thin evaporated layers, it is evident that in the latter cases, some sputtering was initiated by ions which passed into the substrate. If there were discontinuities present at the interface, such as would be introduced by adsorbed gas on the substrate during evaporation, the passage of focusons to the surface would be affected. The most likely effect of a lattice defect would be to stop, or to scatter the focuson, thus producing a cosine distribution.

These experiments, then, do not seriously challenge the view stated by the model, that the bulk of sputtered atoms originate at the surface. Better experiments of this nature would provide a critical test of the validity of the model.

CONCLUDING REMARKS

The complexity of the interaction between a metal lattice and a beam of energetic ions is evident from the diversity of results obtained under various experimental conditions. Yet these diverse results are in qualitative agreement with a model which gives proper consideration to the interaction of the

³Robinson and Oen (ref. 35) have recently discovered a phenomenon termed "channeling" or "tunnel focusing", where, in certain cases, crowdions are able to travel in the close-packed directions for distances on the order of focuson ranges or longer. This phenomenon occurs less than 1 percent of the time, but does explain the exponential tail of certain range curves (ref. 36). Consequently, this contribution to sputtering is neglected here.

lattice structure with the collisions occurring within the lattice. This interaction produces two populations of energetic atoms capable of contributing to sputtering. The first population, the crowdions, replicons, and focusons, is responsible for most of the atoms sputtered and explains such phenomena as single crystal spot patterns, decrease in yield with temperature, etc. The second, or thermal population, composed of atoms at very much lower energies, explains such phenomena as the haze between spots in single crystal spot patterns and the behavior of the mean kinetic energy of sputtered atoms with ion penetration depth. Thus, although quantitative prediction of sputtering behavior has not yet been achieved, there is reason to believe that this model leads to the correct conclusions as to the nature of the sputtering process. The model successfully clarifies and unifies the diverse distributions of sputtered material obtained experimentally.

Ames Research Center
National Aeronautics and Space Administration
Moffett Field, Calif., Jan. 2, 1964

REFERENCES

1. Bader, M., Witteborn, F. C., and Snouse, T. W.: Sputtering of Metals by Mass-Analyzed N_2^+ and N^+ . NASA TR R-105, 1961.
2. Snouse, T. W., and Bader, M.: The Sputtering of Copper by N_2^+ as a Function of Pressure and Temperature. 1961 Trans., 8th Natl. Vacuum Symp. and 2nd Int. Cong., vol. I, Pergamon Press, New York, 1962, pp. 271-274.
3. Yonts, O. C., and Harrison, D. E., Jr.: Surface Cleaning by Cathode Sputtering. Jour. Appl. Phys., vol. 31, no. 9, Sept. 1960, pp. 1583-1592.
4. Molchanov, V. A., and Tel'kovskii, V. G.: Variation of the Cathode Sputtering Coefficient as a Function of the Angle of Incidence of Ions on a Target. Doklady Akademii Nauk SSSR, vol. 136, no. 4, Feb. 1961, pp. 801-802. (Trans. Sov. Phys. Doklady, vol. 6, no. 2, Aug. 1961, pp. 137-138).
5. Rogers, E. E.: Research on Experimental Evaluation of Sputtering Yields. Progress Rep. 259-3, contract AF 33 (616)-8120, The Marquardt Corp., Jan. 1962.
6. Thommen, K.: Uber die Zerstaubung von Kristallen durch Kanalstrahlen. (Sputtering of Crystals by Positive Ions.) Z. Phys., vol. 151, 1958, pp. 144-158.
7. Almén, O., and Bruce, G.: Collection and Sputtering Experiments With Noble Gas Ions. Nuc. Instr. and Meth., vol. 11, 1961, pp. 257-278.
8. Southern, A. L., Willis, W. R., and Robinson, M. T.: Sputtering Experiments with 1- to 5-kev Ar^+ Ions. Jour. Appl. Phys., vol. 34, no. 1, Jan. 1963, pp. 153-163.
9. Bohr, N.: The Penetration of Atomic Particles Through Matter. Det. Kongelige Danske Videnskabernes Selskab, Matematiskfysiske Meddelelser, vol. 18, no. 8, 1948.
10. Harrison, D. E., Jr.: A Theoretical Model of the Sputtering Process. 1961 Trans., 8th Natl. Vacuum Sym. and 2nd Int. Cong., vol. I, Pergamon Press, New York, 1962, pp. 259-264.
11. Paneth, H.: The Mechanism of Self-Diffusion in Alkali Metals. Phys. Rev. vol. 80, 1950, pp. 708-711.
12. Thompson, D. O., Blewitt, T. H., and Holmes, D. K.: Low Temperature Measurements of the Young's Modulus and Internal Friction of Copper During Irradiation. Jour. Appl. Phys., vol. 28, 1957, pp. 742-3.
13. Liebfried, G.: Defects in Dislocations Produced By Focusing Collision in f.c.c. Lattices. Jour. Appl. Phys., vol. 31, no. 1, Jan. 1960, pp. 117-121.

14. Silsbee, R. H.: Focusing in Collision Problems in Solids. Jour. Appl. Phys., vol. 28, no. 11, Nov. 1957, pp. 1246-1250.
15. Liebfried, G.: Correlated Collisions in a Displacement Spike. Jour. Appl. Phys., vol. 30, no. 9, Sept. 1959, pp. 1388-1396.
16. Harrison, D. E., Jr.: Determination of the Maximum Lattice-Chain Energy from Sputtering Yield Curves. Jour. Appl. Phys., vol. 32, no. 5, May 1961, pp. 924-927.
17. Nelson, R. S., and Thompson, M. W.: Atomic Collision Sequences in Crystals of Copper, Silver, and Gold Revealed by Sputtering in Energetic Ion Beams. Proc. Roy. Soc., ser. A, vol. 259, no. 1299, 1961, pp. 458-479.
18. Baroody, E. M.: Focusing Collisions in a Linear Chain of Atoms. Phys. Rev., vol. 124, no. 3, Nov. 1, 1961, pp. 745-747.
19. Gibson, J. B., Goland, A. N., Milgram, M., and Vineyard, G. H.: Dynamics of Radiation Damage. Phys. Rev., vol. 120, no. 4, Nov. 15, 1960, pp. 1229-1253.
20. Thompson, M. W., and Nelson, R. S.: Evidence for Heated Spikes in Bombarded Gold from the Energy Spectrum of Atoms Ejected by 43 keV A^+ and Xe^+ Ions. Phil. Mag., vol. 7, no. 84, Dec. 1962, pp. 2015-2026.
21. Wehner, G. K.: Controlled Sputtering of Metals by Low Energy Hg^+ Ions. Phys. Rev., vol. 102, no. 3, May 1, 1956, pp. 690-704.
22. Yurasova, V. E., Pleshivtsev, N. V., and Orfanov, I. V.: Directed Emission of Particles from a Copper Single Crystal Sputtered by Bombardment with Ions up to 50 keV Energy. (Trans. Sov. Phys. JETP, vol. 10, April 1960, pp. 689-693)
23. Cassingnol, C., and Ranc, G.: Sur le Caractère non Linéaire en Fonction de l'Intensité de la Pulvérisation Cathodique à haute énergie et sa Variation en Fonction de la Température. (Concerning the non-linearity of sputtering yield at high energy and its dependence on temperature.) Comptes Rendus (Paris), vol. 248, 1959, pp. 1988-1990.
24. Seeliger, R., and Sommermeyer, K.: Bemerkung zur Theorie der Kathodenzerstäubung. (Remarks on the Theory of Cathode Sputtering) Z. Phys., vol. 93, 1935, pp. 692-695.
25. Wehner, G. K., and Rosenberg, D.: Angular Distribution of Sputtered Material. Jour. Appl. Phys., vol. 31, no. 1, Jan. 1960, pp. 177-179.
26. Rol, P. K., Fluit, J. M., and Kistemaker, J.: Sputtering of Copper by Ion-Bombardment in the Energy Range of 5 - 25 keV. Proc. International Symposium on Isotope Separation, North Holland Pub. Co., Amsterdam, 1958, pp. 657-662.

27. Stein, R. P., and Hurlbut, F. C.: Angular Distribution of Sputtered Atoms. Phys. Rev., vol. 123, no. 3, Aug. 1, 1961, pp. 790-796.
28. Patterson, H., and Tomlin, D. H.: Experiments by Radioactive Tracer Methods on Sputtering by Rare-Gas Ions. Proc. Roy. Soc., ser. A, vol. 265, no. 1323, Feb. 6, 1962, pp. 474-488.
29. Grönlund, F., and Moore, W. J.: Sputtering of Silver by Light Ions with Energies from 2 to 12 keV. Jour. Chem. Phys., vol. 32, no. 5, May 1960, pp. 1540-1545.
30. Pleshivtsev, N. V.: Sputtering of Copper by Hydrogen Ions with Energies up to 50 keV. J. Exptl. Theoret. Phys. USSR, vol. 37, Nov. 1959, pp. 1233-1240. (Trans. Sov. Phys. JETP, vol. 10, no. 5, May 1960, pp. 878-883)
31. Bulgakov, Yu. V.: On N. V. Pleshivtsev's Article, "Sputtering of Copper by Hydrogen Ions with Energy up to 50 keV." (Trans. Sov. Phys. JETP, vol. 14, no. 6, June 1962, p. 1431)
32. O'Briain, C. D., Lindner, A., and Moore, W. J.: Sputtering of Silver by Hydrogen Ions. Jour. Chem. Phys., vol. 29, no. 1, July 1958, pp. 3-7.
33. Dushikov, I. I., Molchanov, V. A., Tel'kovskii, V. G., and Chicherov, V. M.: "Some Angular Relations Associated With Cathode Pulverization." Zhurnal Tekh. Fiz., vol. 31, no. 8, Aug. 1961, p. 1012. (Trans. Sov. Phys. Tech. Phys., vol. 6, no. 8, Feb. 1962, p. 735)
34. Kopitzki, and Stier, H.: Mittlere Kinetische Energie der bei der Kathodenzerstäubung von Metallen ausgesandten Partikel. (Mean Kinetic Energy of Particles Sputtered from Metals). Z. Naturforschg. vol. 17a, 1962, pp. 346-352.
35. Robinson, M. T., and Oen, O. S.: The Channeling of Energetic Atoms in Crystal Lattices. Applied Physics Lttrs., vol. 2, no. 2, Jan. 15, 1963, p. 30.
36. Davies, J. A., and Sims, G. A.: The Range of Na^{24} Ions of Kiloelectron Volt Energies in Aluminum. Can. Jour. Chem., vol. 39, 1961, pp. 601-610. Also Can. Jour. Chem., vol. 38, 1960, pp. 1535-1546.
37. Van Lint, V. A. J., Schmitt, R. A., and Suffredini, C. S.: Range of 2- to 60-keV Recoil Atoms in Cu, Ag, and Au. Phys. Rev., vol. 121, no. 5, March 1, 1961, pp. 1457-1463.

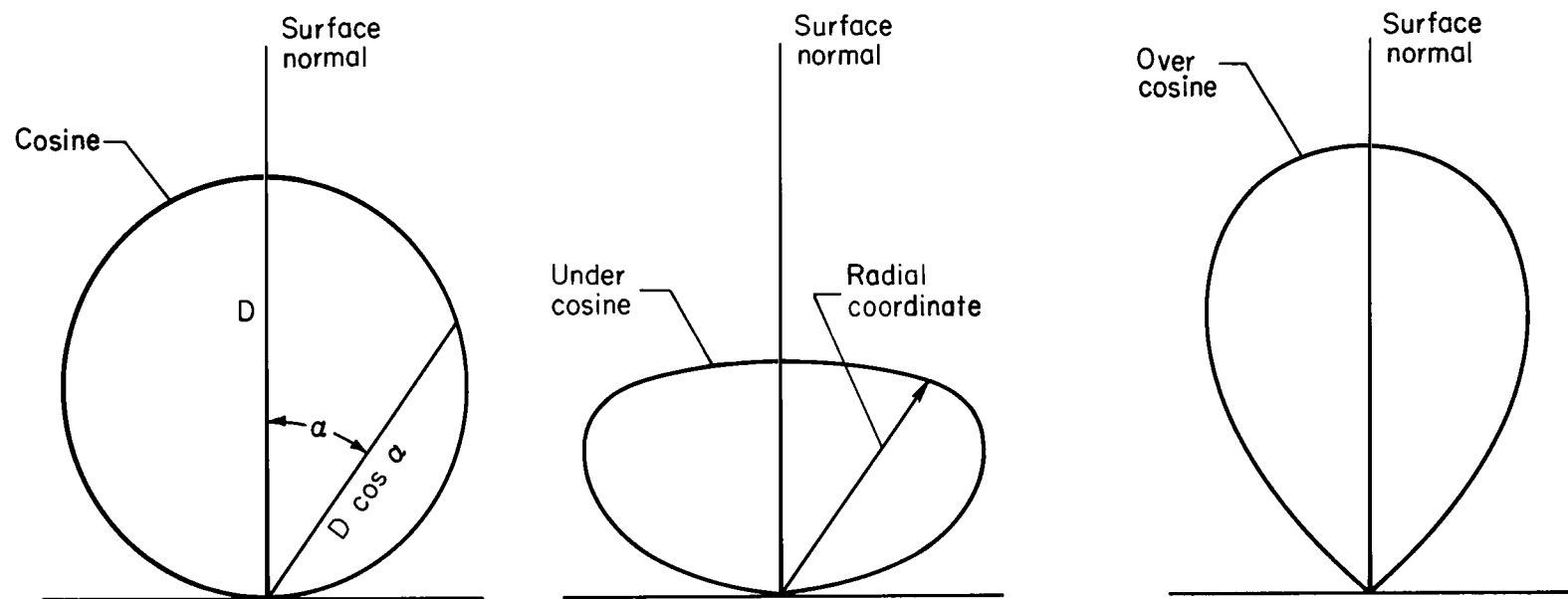


Figure 1.- Definition of cosine, under cosine, and over cosine distributions.

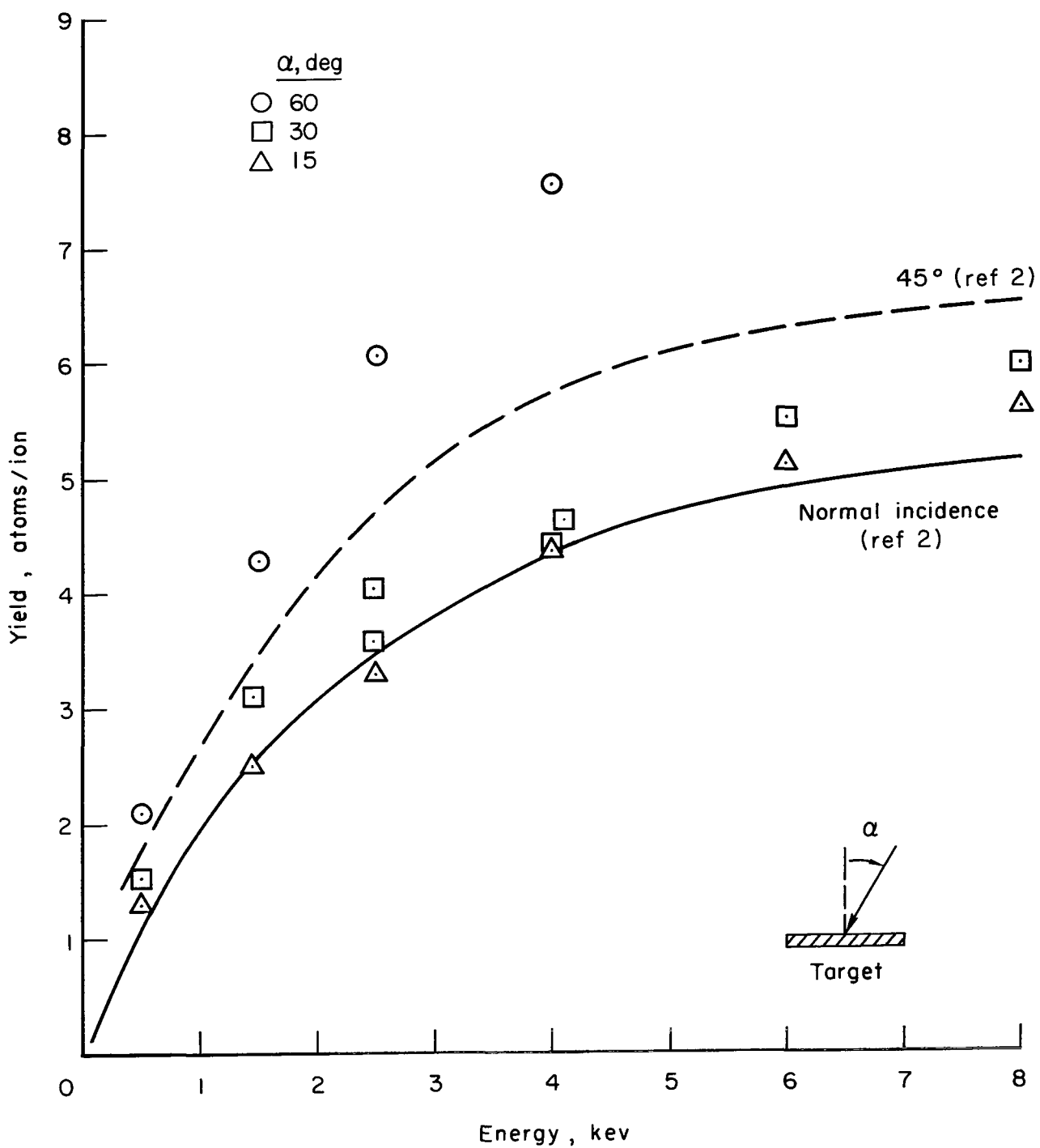


Figure 2.- Sputtering yield of polycrystalline copper sputtered by N_2^+ ions as a function of energy and angle of ion incidence.

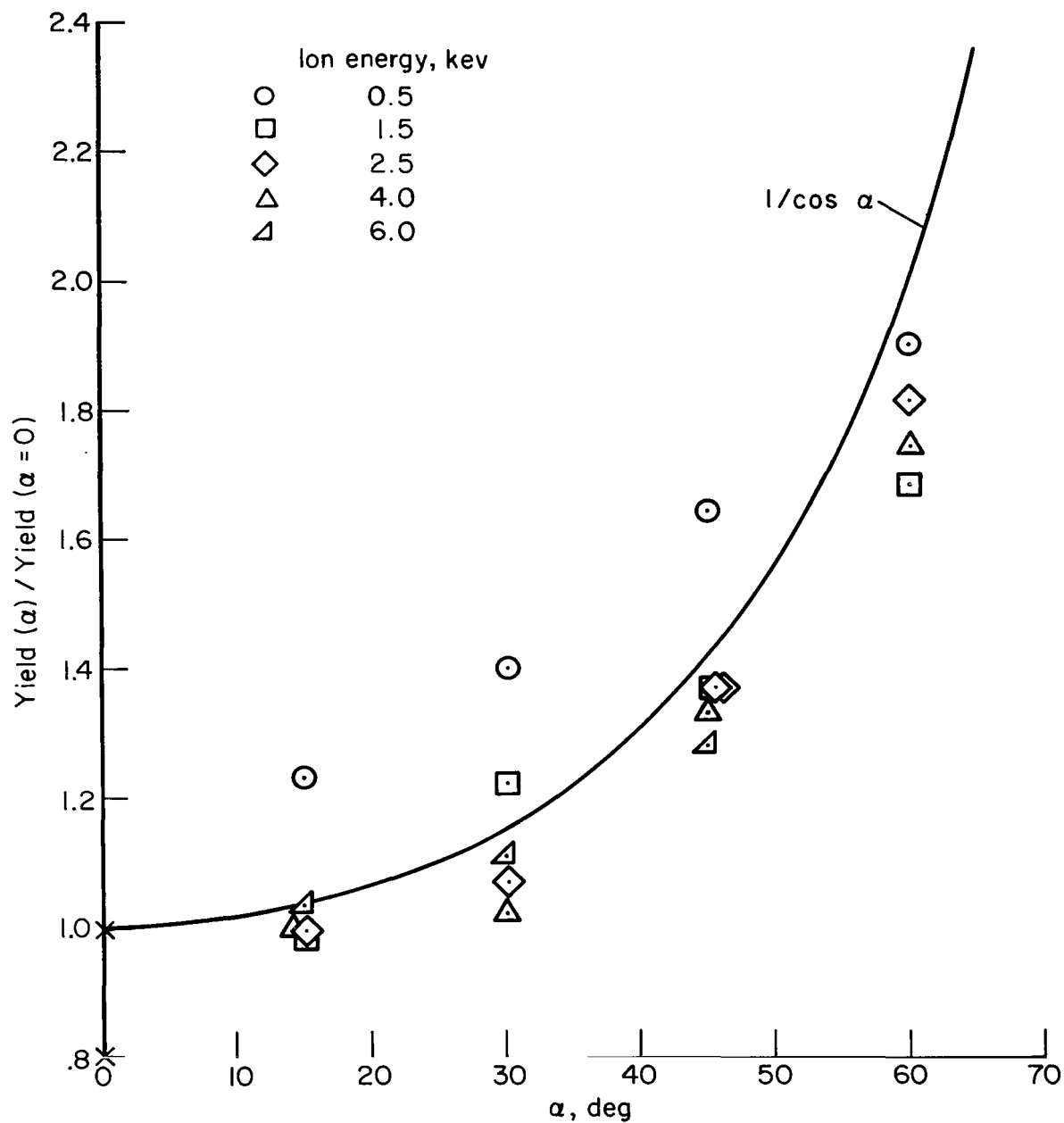


Figure 3.- Ratio of oblique to normal incidence angle yields of copper sputtered by N_2^+ at various energies.

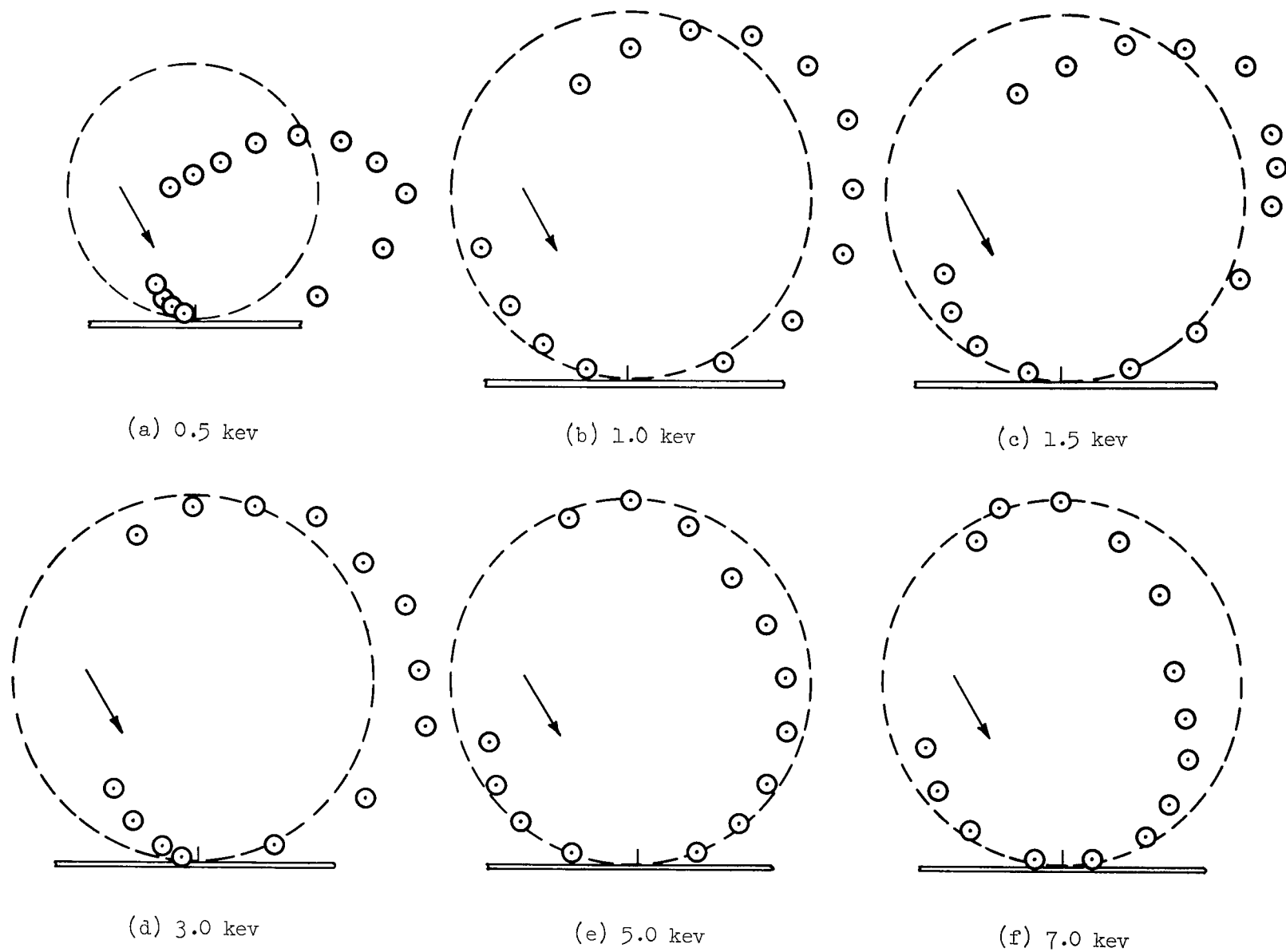
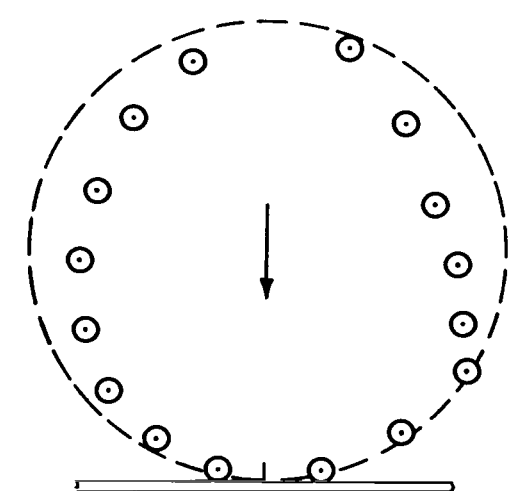
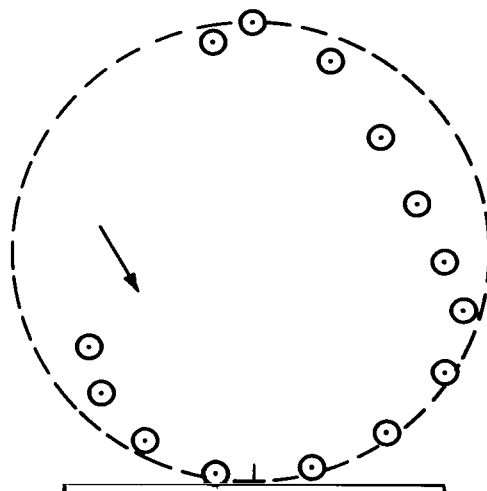


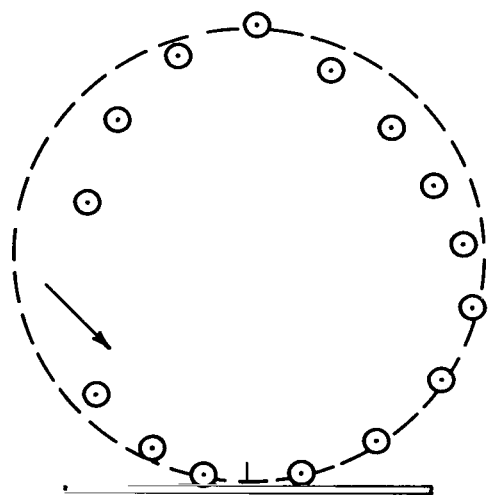
Figure 4.- Angular distribution of polycrystalline copper sputtered by N_2^+ at $\alpha = 30^\circ$. Radial coordinate indicates relative deposit density.



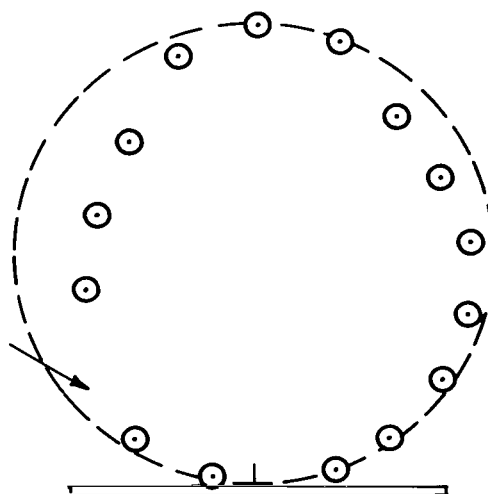
(a) $\alpha = 0^\circ$



(b) $\alpha = 30^\circ$

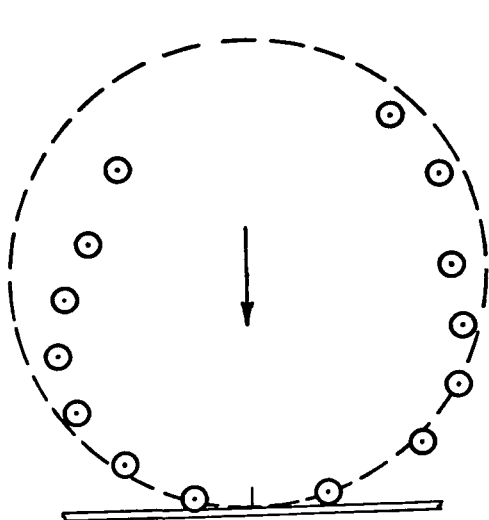


(c) $\alpha = 45^\circ$

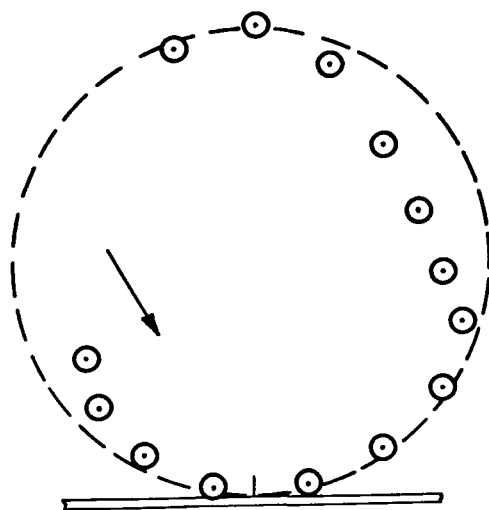


(d) $\alpha = 60^\circ$

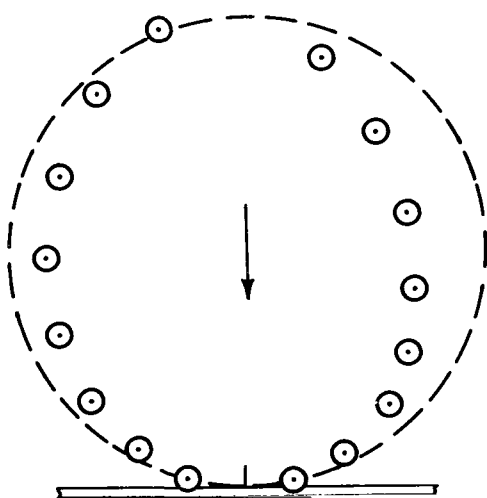
Figure 5.- Angular distribution of polycrystalline copper sputtered by 4 kev N_2^+ .



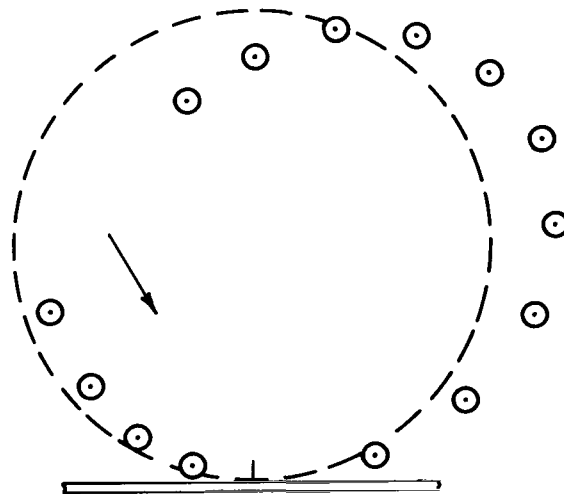
(a) 6 keV N_2^+ ions at 0° incidence.



(b) 4 keV N_2^+ ions at 30° incidence.



(c) 5 keV N^+ ions at 0° incidence.



(d) 1 keV N_2^+ ions at 30° incidence.

Figure 6.- Comparison of angular distributions.

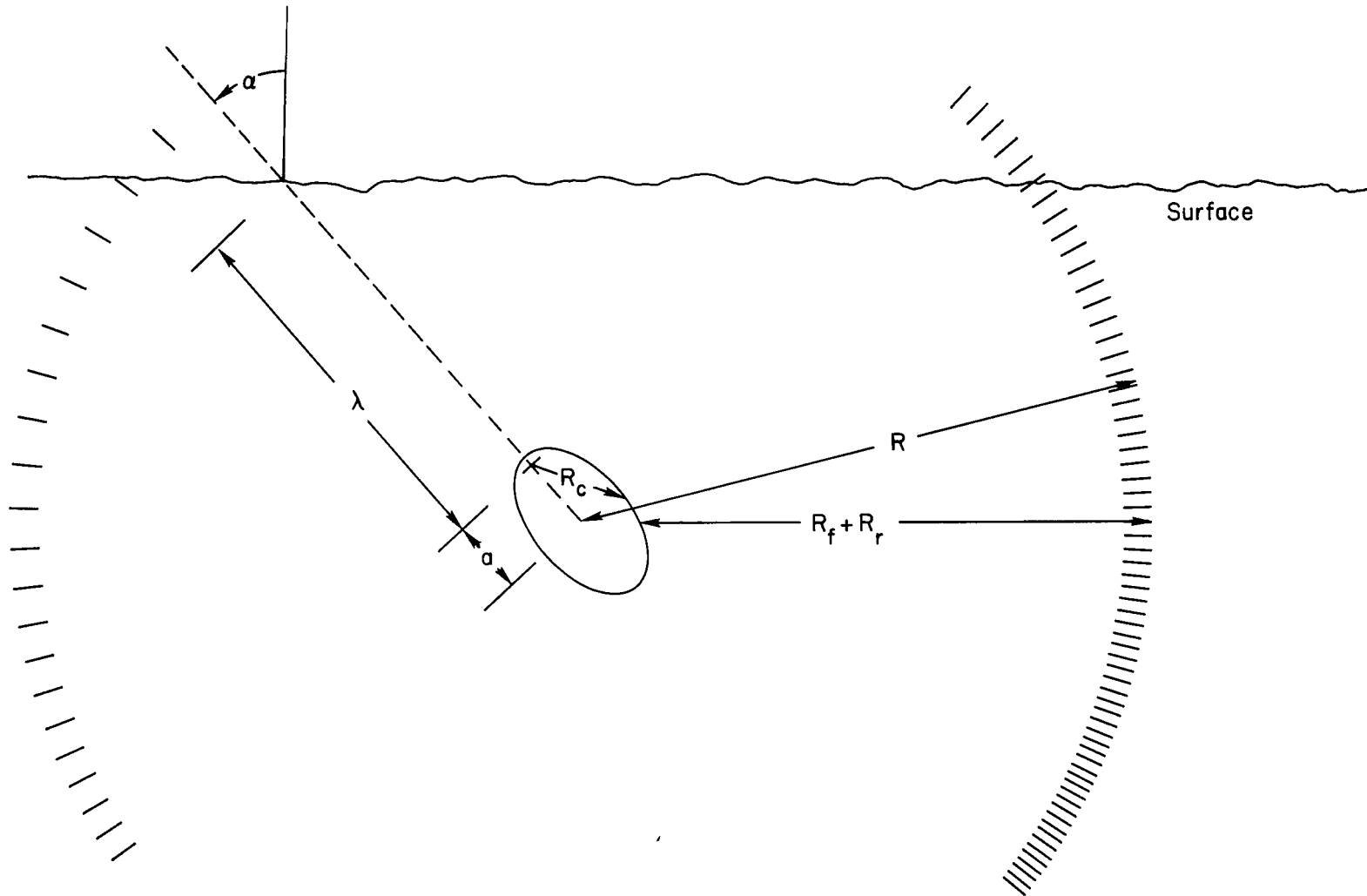


Figure 7.- Schematic drawing of the sputtering process (medium energies).

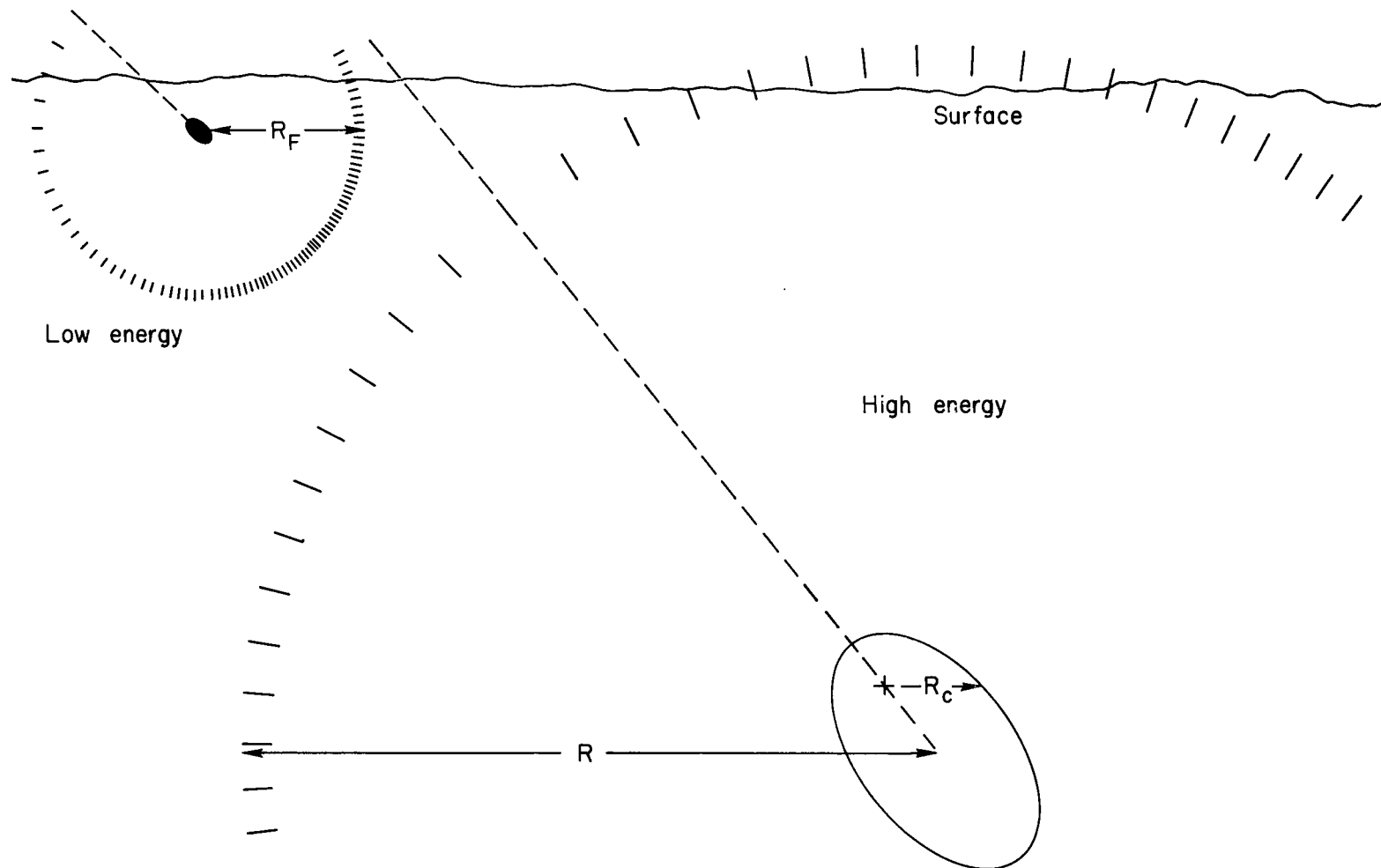


Figure 8.- Schematic drawing of polycrystalline sputtering.

2/17/25
92

"The National Aeronautics and Space Administration . . . shall . . . provide for the widest practical appropriate dissemination of information concerning its activities and the results thereof . . . objectives being the expansion of human knowledge of phenomena in the atmosphere and space."

—NATIONAL AERONAUTICS AND SPACE ACT OF 1958

NASA SCIENTIFIC AND TECHNICAL PUBLICATIONS

TECHNICAL REPORTS: Scientific and technical information considered important, complete, and a lasting contribution to existing knowledge.

TECHNICAL NOTES: Information less broad in scope but nevertheless of importance as a contribution to existing knowledge.

TECHNICAL MEMORANDUMS: Information receiving limited distribution because of preliminary data, security classification, or other reasons.

CONTRACTOR REPORTS: Technical information generated in connection with a NASA contract or grant and released under NASA auspices.

TECHNICAL TRANSLATIONS: Information published in a foreign language considered to merit NASA distribution in English.

TECHNICAL REPRINTS: Information derived from NASA activities and initially published in the form of journal articles or meeting papers.

SPECIAL PUBLICATIONS: Information derived from or of value to NASA activities but not necessarily reporting the results of individual NASA-programmed scientific efforts. Publications include conference proceedings, monographs, data compilations, handbooks, sourcebooks, and special bibliographies.

Details on the availability of these publications may be obtained from:

SCIENTIFIC AND TECHNICAL INFORMATION DIVISION
NATIONAL AERONAUTICS AND SPACE ADMINISTRATION

Washington, D.C. 20546